5-2019

Vector Flow Imaging in Pediatric Cardiology - Extracting and Validating Data

Mason Belue

UNIVERSITY OF
ARKANSAS
HONORS COLLEGE

Vector Flow Imaging in Pediatric Cardiology – Extracting and Validating Data

Bachelor of Science in Biomedical Engineering

Mason Belue

May 2019

University of Arkansas

Honors Advisors: Dr. Morten and Hanna Jensen

Graduate Student Advisor: Megan Laughlin

Abstract

In the field of bedside cardiac diagnostic imaging, Doppler Ultrasound (DU) is the gold standard for diagnosing heart conditions. The largest benefit of DU is its ability to noninvasively image cardiac flow and allow the estimation of blood velocity and quantification of anatomical disease. However, to get correct velocity estimation, the position of the transducer in relation to the flow field needs to be known. This is the problem of angle/direction dependency and limits DUs accuracy when imaging in areas where perfect alignment or exact position of the transducer in relation to flow field is not possible or known, such as in the left ventricle. As a solution to the problem of angle dependency, Vector Flow Imaging (VFI) is used because it is non-invasive and angle-independent. In this study, VFI was used in 12 pediatric patients from Arkansas Children's Hospital to analyze left ventricular flow using the 4-chamber view. The shape, in the form of ellipse Major:Minor axis ratio, of ventricular vortices was then measured. The deviation of an individual patients heart flow from what is theoretically healthy as defined in literature, an ellipse with Major:Minor axis ratio of 1.9, was compared to what was measured with VFI. The average directional deviation for these 12 patients was $64.85^{o} \pm 10.34^{o}$ from what is theoretically healthy. After optimizing ellipse parameters to actual patient flow, the true average optimal ratio was found to be 1.98 ± 0.58. Additionally, it was found that heart rate ($p < 0.0001$), age ($p = 0.003$), and weight ($p < 0.0001$) had a significant effect on angle deviation. However, there was no trend in the data. This preliminary study paves the way for using VFI to define healthy parameters for left ventricular flow and assist clinicians with more accurate diagnoses in anatomical areas with complex flow.

Table of Contents

1 Background

1.1 Motivation

Congenital heart disease (CHD) accounts for nearly one-third of all major congenital anomalies (Linde 2011). The incidence of CHD, in both moderate and severe forms, is about 6 in 1,000 live births, and of all forms increases to 75 in 1,000 live births if trivial lesions and ventricular septal defects are included (Hoffman 2002). In children with CHDs, Doppler ultrasound is the gold-standard imaging modality for noninvasive bedside imaging. However, due to the angle-dependent and one-dimensional velocity estimations of Doppler ultrasound, precise characterization of blood flow is nearly impossible (Collins 2019). Additionally, the need for complex and precise flow analysis is growing as wall motion abnormalities, manifesting itself as disturbed vortical blood flow, could signal the presence of maladaptive function even before noticeable structural changes arise. This could reveal preclinical disease or physiologically unstable conditions that can lead to left ventricular remodeling and clinical heart failure (Pedrizzetti 2014). Vector Flow Imaging (VFI) can be utilized in pediatric cardiac cases where real-time noninvasive angle-independent visualization of complex flow is needed, providing advanced detail of blood flow patterns within the cardiac chambers, across valves, and in the great arteries (Collins 2019).

1.2 Left Ventricular Physiology and Significance of Vortical Flow

Left ventricular ejection is based on the concept of low-pressure filling, which is initiated by a heart phase known as isovolumetric relaxation (Pedrizzetti 2014). During isovolumetric relaxation, both the mitral valve and the aortic valve are closed while the left ventricle relaxes, increasing in volume and decreasing in pressure. After this isovolumetric relaxation phase, the

mitral valve opens and blood flows from the left atrium to the ventricle entirely from the apical suction force driven by pressure differences between the atrium and ventricle. This phase together with an untwisting feature enhances the elastic recoil of potential energy stored in the myocardium during ventricular contraction (Pedrizzetti 2014). As blood is filling the ventricle after isovolumetric relaxation, a ring-shaped region of rotating flow motion, known as vortices, forms. Mathematically, vorticity physically coresponds to (twice) the local angular velocity of a fluid particle. A shear layer is an elongated layer of vorticity (Sengupta 2012). These vortices are recirculating flows beneath the valve leaflets, where the dominant direction being under the free edge of the anterior mitral leaflet towards the aorta, also known as towards the outflow tract (Figure 1). Additional transient recirculation is also seen beneath the posterior mitral valve leaflet (Kilner 2000). This vorticity does not form spontaneously in a flow field but instead develops because of the velocity difference between the inflow and the adjacent boundary layer (Sengupta 2012). The layer in between the two flows is called a shear layer, also being characterized by high shear friction between the two flows of differing velocities (Pedrizzetti 2014).

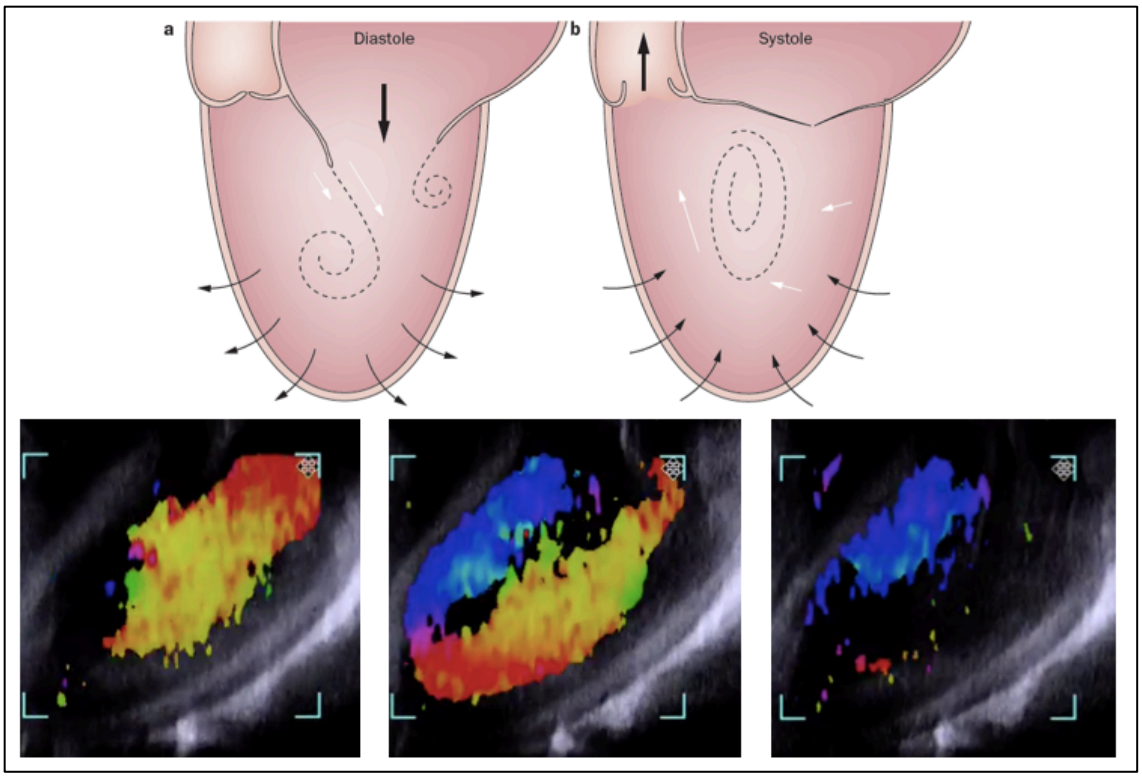

Figure 1 Vortical flow seen throughout the cardiac cycle from diastole to systole in the 4-chamber view (Sengupta 2012).

It is suggested that the swirling of blood in the left ventricle, although potentially associated with a higher wall shear stress, might avoid excessive energy dissipation by limiting flow separation and instability (Kilner 2000). This subsequently decreases the amount of energy that the myocardial muscle must produce to eject the blood into the primary circulation. Any disruption of this natural arrangement results in an increase in the work required by the heart to eject blood into circulation, thus activating additional chemical work and augmenting oxygen consumption (Pedrizzetti 2005). Owing to the special conditions which give rise to vorticies, it is evident that minor modifications in the surrounding conditions will lead to large differences in energetic and possibly dynamic properties of cardiac flow. Flow analysis of these energetic and dynamic deviations can reveal small modifications in left ventricular function before ventricular tissues have undergone clinically relevant changes in mechanical properties (Pedrizzetti 2014).

Disrupted left ventricular fluid mechanics is characterized by two main factors: 1) Vortex instability originating from irregular shear stress resulting in substantial increases in energy dissipation and poor energetic performance and 2) the vortex instability from irregular shear stress also leading to deviations from normal intraventricular pressure gradients (Pedrizzetti 2014). Various heart conditions and their results on ventricular flow can be seen in figure 2. Thus, analysis and characterization of vortical flow can help differentiate between healthy and diseased hearts and, additionally, show dynamic pathologies which have not yet resulted in mechanical problems. Serving as both a diagnostic and predictive analytic tool for pediatric cardiac patients.

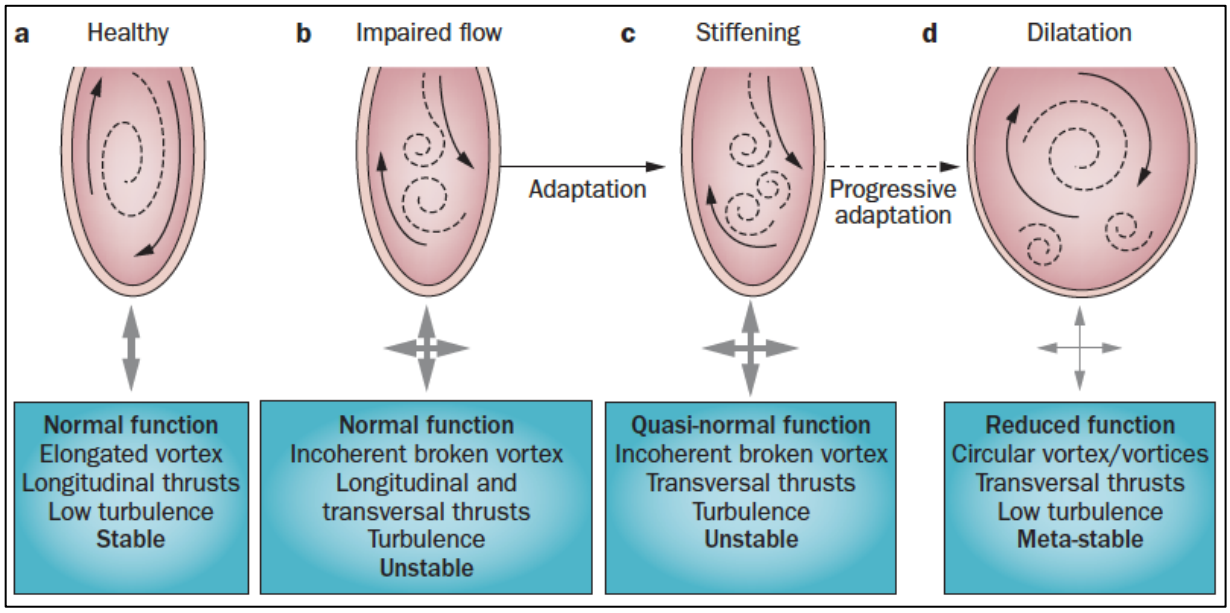

Figure 2: The result on vortical flow from different stages of left ventricular remodeling (Pedrizzetti 2014).

1.3 Vector Flow Imaging

Vector Flow Imaging (VFI) is an ultrasound-based imaging technique that provides real-time, angle-independent visualization of flow (Collins 2019). VFI assesses the movement of the object from a field with spatial oscillations in both the axial direction of the transducer and in

one direction transverse to this axial direction (Munk 1998). It assesses both the transverse and axial velocity components simultaneously via an optical filtering technique known as dual-peaked receiver apodization (Collins 2019). Commercially available VFI transducers have a penetration depth of 5cm, limiting the use to superficial flow (Hansen 2015). Increasing penetration depth increases the error of the transverse velocity estimate, mainly governed by the distance between the peaks of the two-point source receiving apodization function (Hansen 2015). Although absolute velocity magnitude is impaired at increasing penetration depths, there has not been anything mentioned in the literature about direction impairment. In some studies (Collin 2019), adequate penetration was obtained to a depth of 6.5cm without compromising the ability to readily identify cardiac anatomy and observe cardiac blood flow (Collins 2019).

This is much different from conventional doppler ultrasound, which can only give information about velocity in the axial direction from the transducer. A conventional doppler pulse is emitted and the scattered motion is then tracked along two orthogonal axes (Hansen 2015). The displacement between the two scattering signals in time, which is due to the movement of the blood between pulse emissions, allows for velocity estimation (Munk 1998). Because velocity is only assessed in the axial direction, velocity components which are perpendicular to the beam propagation will not be measured, resulting in velocity underestimation.

One common limitation which both 2D doppler and 2D VFI have is that they both ignore the flow through the 2D plane being measured in the third dimension. This error introduced is on the order of 15% for healthy hearts (Sengupta 2012). Another limitation of VFI is the very small

penetration depth of VFI of 5cm, severely limiting the applications for its use (Collins 2019). The major assumption of VFI is that all the flow along each radius within an image can be deconstructed into laminar flow with a vortical component with a zero mean. The transverse velocity is computed assuming that the vortical component of flow satisfies the continuity equation from pixel to pixel and across all the scan lines in the field of the color flow image (Sengupta 2012). One of the greatest advantages of using VFI is the lack of anesthetization required as a bedside imaging modality. This is particularly advantageous in patients with more complex conditions, such as those with Williams syndrome, who have a greater risk of experiencing adverse effects to anesthesia (Collins 2019). Another advantage of VFI is its noninvasiveness and its rapid scan time as compared to flow MRI, particle image velocimetry, and many more (Collins 2019, Sengupta 2012).

2 Materials and Methods

2.1 Patients Protocol and VFI Setup

The University of Arkansas for Medical Sciences Institutional Review Board approved the human portion of the study and thus the protocol conformed to all ethical guidelines. All patient information was de-identified and stored in a secured location. Informed consent was obtained for all participating patients. The patients were studied using a BK Ultrasound bk5000 system with built-in vector flow imaging (BK Medical, Peabody, MA) equipped with a 5MHz linear probe (Linear Array 8 I.2, BK Medical) to perform transthoracic echocardiography. Transthoracic imaging was performed sequentially from parasternal long-axis and short-axis, apical, and 4-

chamber views. All scan settings, such as pulse repetition frequency, frequency, and thus velocity range, were optimized for each patient, as seen on all the videos.

2.2 Overall Angle Calculation

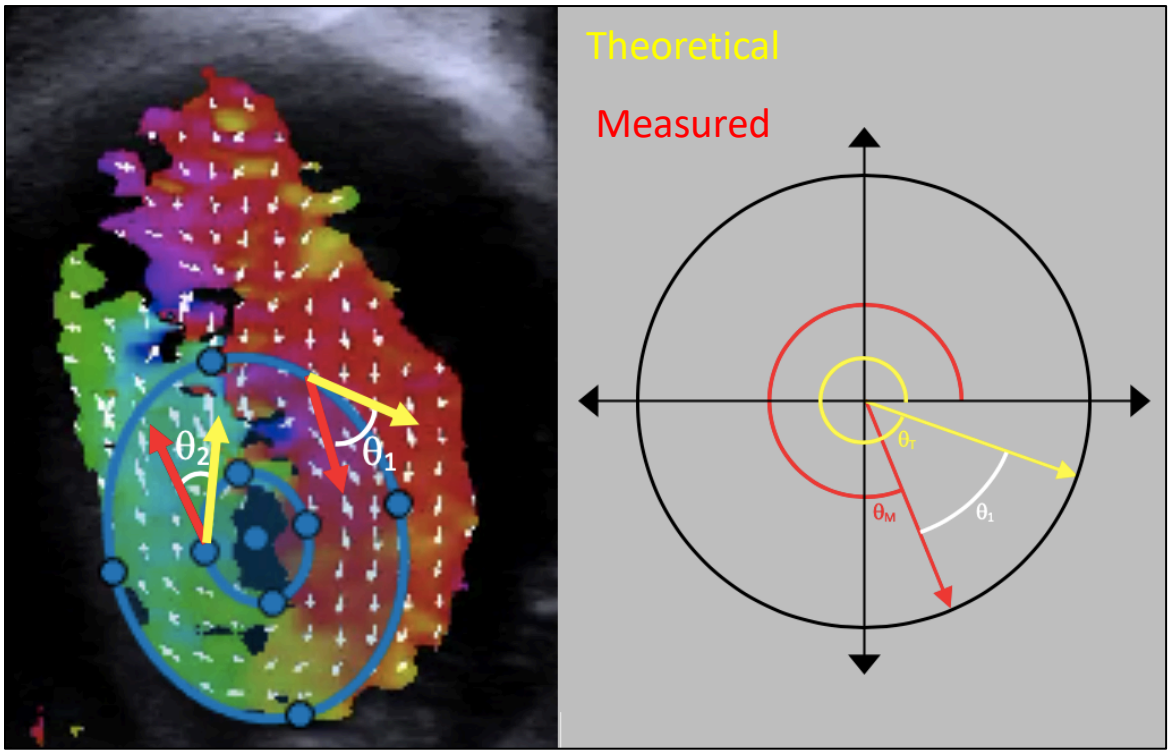

Figure 3: Overall angle deviation calculation for the comparison of measured direction and theoretical (healthy) direction

To measure the deviation between the theoretical flow direction (based off of a healthy heart) and the measured direction, the difference is taken between the two directions (Figure 3). The theoretical flow direction is defined as the tangent to an ellipse at a particular [x, y] along the ellipse. The ellipse major and minor axes are defined by literature values for healthy hearts and the aspect ratio is maintained through MATLAB image analysis. The measured flow is found through analysis of the hue values of the pixel at position [x, y] which gives the direction with respect to a color wheel. Any corrections for VFI color wheel orientations which are different from the HUE wheel are made within the code. Any corrections for the theoretical angle

calculation are also made in the code. Calculation of both the theoretical and measured directions are described in depth below.

2.3 Calculation of Measured Angle

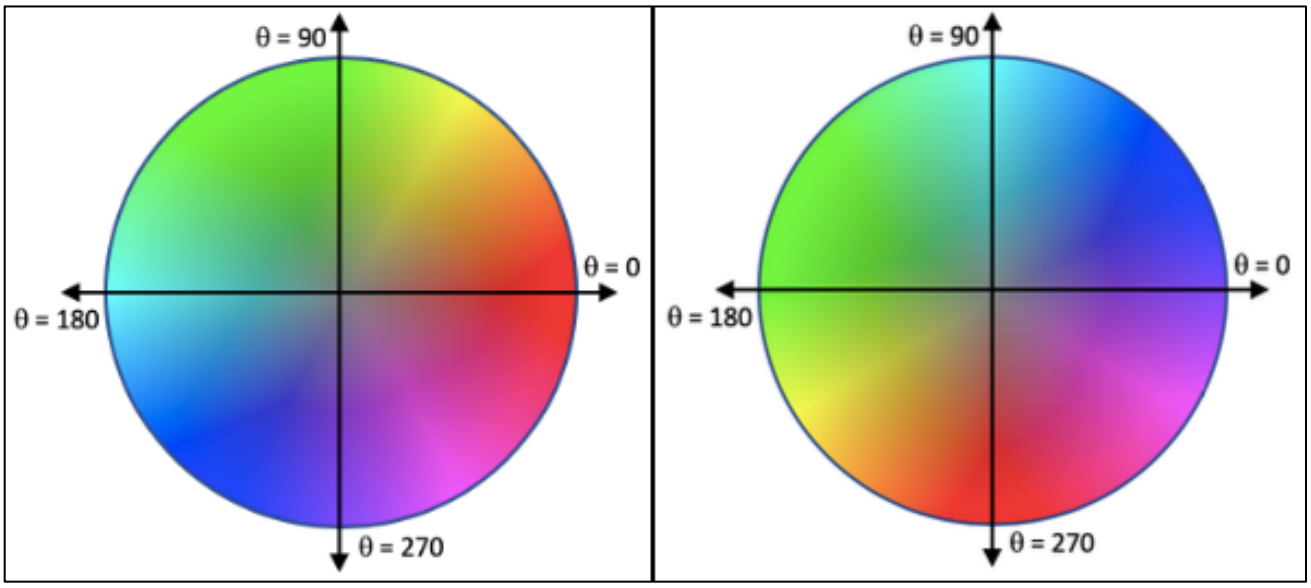

Figure 4: HSL color wheel adjusted for VFI reference directions. Image on left of uncorrected HSL color wheel, image on right is corrected for VFI video differences. For this particular example, the VFI reference square was both flipped over the y-axis and then rotated 90 degrees. This serves as one example of how the HSL color wheel might be corrected for VFI display differences, this is not an exhaustive correction.

Calculating the direction of the measured flow begins first by converting the VFI video data type from RGB to HSV. The hue component of HSV is used to find the direction of flow. In most cases, the hue color wheel will have to be corrected to match the orientation of the VFI reference color square (Figure 4). Conversion of RGB to HSV, and all corrections, are performed with built-in MATLAB functions.

2.4 Calculation of Theoretical Angle

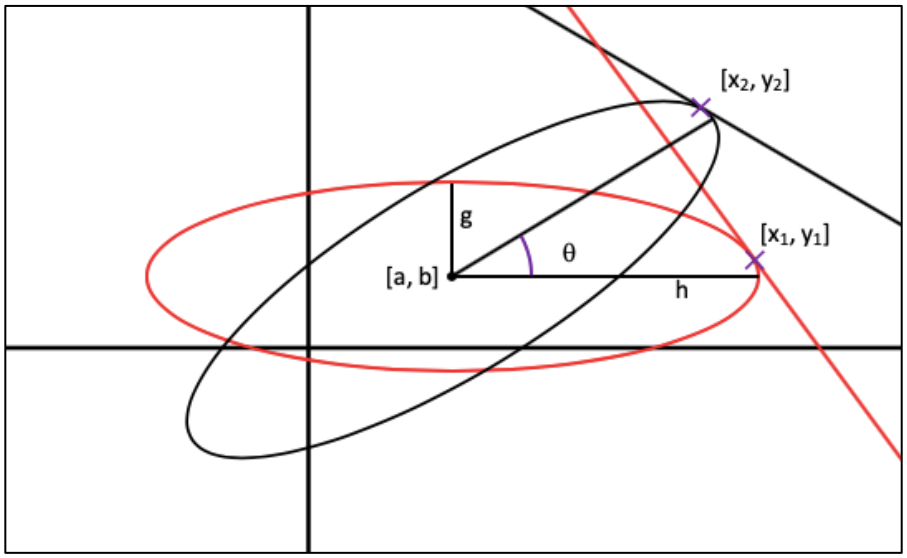

Figure 5: Rotated ellipse at angle θ and offset from origin of [a, b]

The slope of the tangent at point [x_1, y_1] of the non-rotated ellipse is given by the following equation.

$$S_1 = -\frac{dx}{dy} * \frac{g^2}{h^2} = \frac{x_1 - a}{y_1 - b} * \frac{g^2}{h^2}$$

Where [a, b] is defined as the [x, y] offset of the ellipse from origin and [h, g] is the major and minor axis of the ellipse respectively. To get the tangent at point [x_2, y_2] of the rotated ellipse, the position [x_1, y_1] in terms of [x_2, y_2] and θ needs to be obtained. This is done as follows.

$$x_1 = (x_2 - a) * \cos\theta + (y_2 - b) * \sin\theta + a$$

$$y_1 = (y_2 - b) * \cos\theta - (x_2 - a) * \sin\theta + b$$

Then the new transformed [x_1, y_1] is plugged into equation (1) to give the slope of the unrotated ellipse in terms of the point and rotation of the second ellipse.

$$S_1 = \frac{(x_2 - a) * \cos\theta + (y_2 - b) * \sin\theta}{(y_2 - b) * \cos\theta - (x_2 - a) * \sin\theta} * \frac{g^2}{h^2}$$

The slope at point [x_2, y_2] of the rotated ellipse is then given by the following.

$$S_2 = \frac{dy_2}{dx_2} = \frac{S_1 \cos\theta + \sin\theta}{\cos\theta - S_1 * \sin\theta}$$

Taking the inverse tangent of this slope gives the angle or direction of every point along the ellipse, outputting angles between -90 and 90 degrees. Figure 6A gives the general output of angles along an unrotated ellipse.

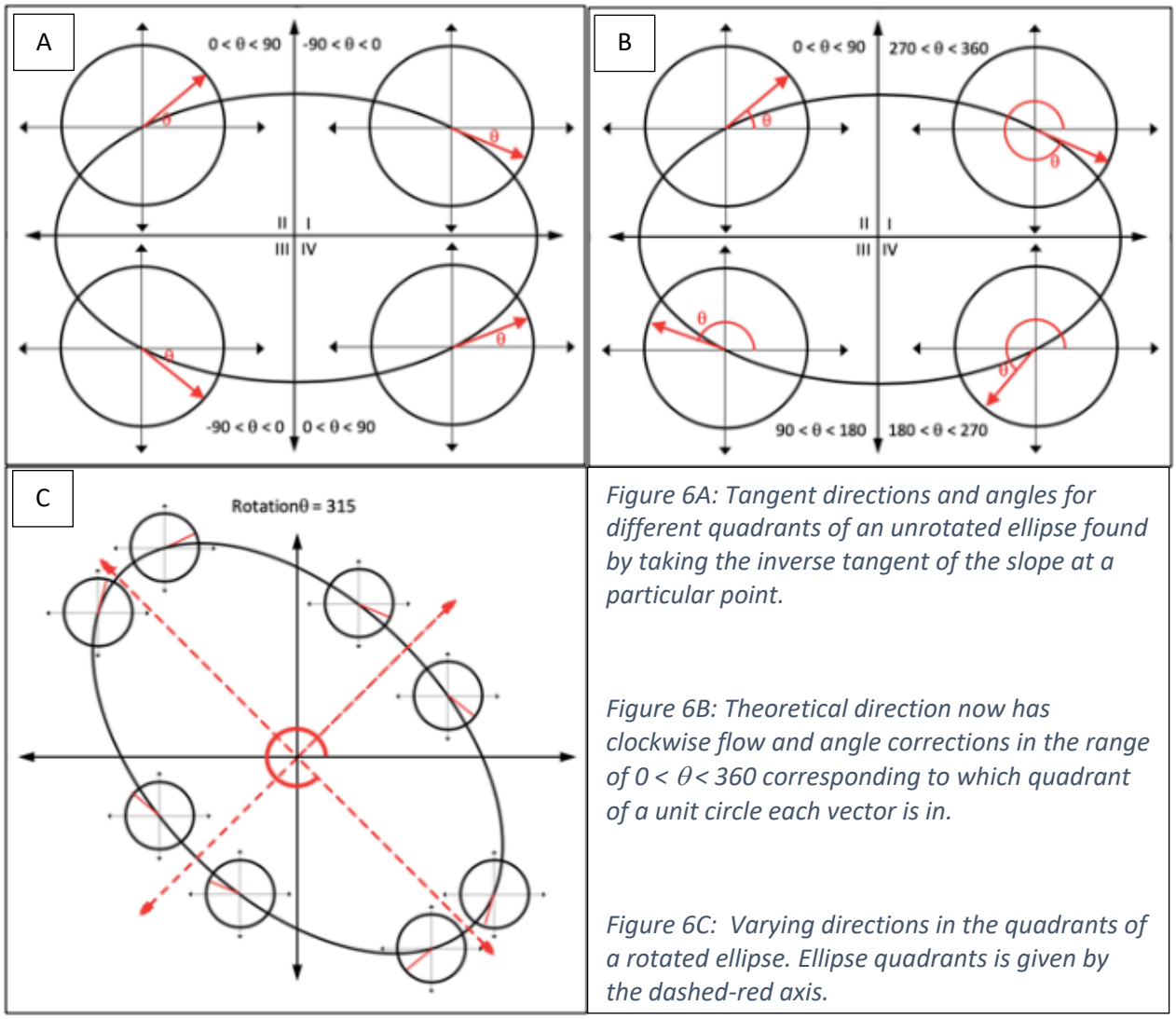

Figure 6A: Tangent directions and angles for different quadrants of an unrotated ellipse found by taking the inverse tangent of the slope at a particular point.

Figure 6B: Theoretical direction now has clockwise flow and angle corrections in the range of $0 < \theta < 360$ corresponding to which quadrant of a unit circle each vector is in.

Figure 6C: Varying directions in the quadrants of a rotated ellipse. Ellipse quadrants is given by the dashed-red axis.

Of special note is how the angles in Figure 6A are only given in the range of $-90 < \theta < 90$ for every point along the ellipse, even when the absolute angles might be in the 4th quadrant (270

$< \theta < 360$). Another special note is how the directions of the theoretical flow vectors are not either all clockwise or counter-clockwise, which would be the case for elliptical blood flow. Both of these points are problematic when trying to compare the measured angles in the range of $0 < \theta < 360$ with non-directional theoretical flow vectors. Therefore, this must be corrected for to result in Figure 6B.

Although the clockwise flow direction and angle range of $0 < \theta < 360$ in Figure 6B has now been calculated, this model is still only derived for a non-rotated ellipse. A rotated ellipse has a few extra considerations which can be best understood by first understanding some basics from Figure 6B. First off, consider the individual ellipse quadrants. Considering quadrant 1, no matter where the point is along the ellipse in this quadrant, the direction will always be within the angle range of $270 < \theta < 360$. The same can be said for every other ellipse quadrant, with the angle range for that quadrant being confined to a specific range. Secondly, the data which is used to define the vertices of the ellipse always starts at the intersection between the 1^{st} and 4^{th} quadrants of the ellipse, for both rotated and unrotated ellipses, and then is swept counter clockwise. When rotating an ellipse, the first point made here is no longer true. In a single ellipse quadrant, the vectors will always be in two different quadrants (i.e. directions). This phenomenon is shown in Figure 6C.

When performing the 6A to 6B switch, this varying quadrant direction can be corrected for by picking either the first, second, third, or fourth, $1/4^{th}$ of the data which corresponds to a single quadrant of the ellipse, and then scrutinizing which directions are positive and which are negative. The directional sign differences, in addition to an understanding of the rotation of the ellipse, will help in the final conversion of Figure 6A to Figure 6C.

3 Results

Table 1: Healthy Human Patient data from vortical flow analysis

Patient	Heart Rate	Weight (kg)	Age (weeks)	Angle Deviation	Optimal Ratio
2	143	4.65	11	43.8	1.85
3	139	3.1	1.14	49.3	2.13
4	116	8.6	21.73	68.8	2.14
5	N/A	3.2	8.69	88.7	2.02
6	144	4.4	8.69	42.4	2.06
7	148	4.25	5	42	1.73
8	140	4.2	0.86	83.2	2.11
9	131	7.8	17.38	68.2	1.76
10	140	3.8	4.35	76.4	2
11	139	3.4	4.35	74.2	2.05
12	148	3.95	1.57	64.6	2.13
13	146	5.05	5	76.6	1.77
				Average Angle Deviation	**Average Optimal Ratio**
				64.85	1.979166667

Using the MATLAB code described above, the average angle deviation for 12 healthy patients was found to be $64.85^{o} \pm 10.34^{o}$ and the average optimal ratio was found to be 1.98 ± 0.58. It was also found that heart rate ($p < 0.0001$), age ($p = 0.003$), and weight ($p < 0.0001$) did have a significant effect on angle deviation. However, there was no trend in the data.

4 Discussion

It is expected that patients who are not healthy, being defined as having some cardiac anomaly leading to disturbed flow, will have greater average angle deviations. It is also suspected that the average optimal ratio will change with unhealthy patients, some studies have suggested that the average optimal ratio will be closer to 1, indicating more circular flow as disease progresses (Collins 2019). Comments on comparing diseased flow to healthy flow cannot be made at this time due to not having data for unhealthy patients.

There was a lot of variability seen within the data, as indicated from the high standard deviations between the angle deviations and optimal ratio for each patient. This variability likely comes because of two reasons: 1) Variability from the ultrasound technician, and 2) between-user variability from the user interface. The first source of variability from the ultrasound technician comes from the need to optimize scan parameters for each patient. These scan parameters include the B Gain, C Gain, and resolution/Hz which all influence the quality of the VFI image as seen in Figure 7. Currently it is impossible to tell if the deviations between patients is due to patient anatomy variation, or whether it is due to the data itself because of the different scan settings. Further analysis and VFI videos will be needed to quantify the full effect of the scan setting nuisance variable.

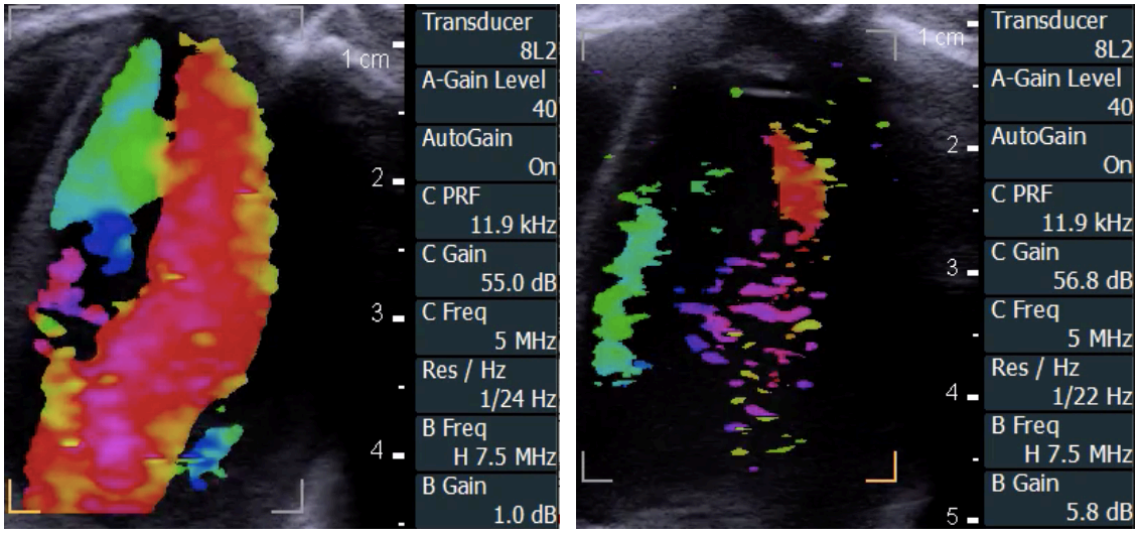

Figure 7: 4-chamber VFI videos from two different patients where different VFI settings are used in each case. It is evident which settings give better images qualitatively.

The second source of between-user variability stems from the inconsistencies of user inputs. Given a single frame that every user has selected to analyze, the various user inputs which lead to data variability are the following: 1) ellipse center point, 2) ellipse rotation indicating flow direction, and 3) bounds for flow analysis. All three of these sources of between user variability cannot be controlled for as each user will have a different interpretation of where the center of flow is and at what direction the flow is heading. Even with the exact same user and the exact same interpretation, it is unlikely that the exact rotation and center point position will be picked again which would lead to differences in the data. Post-analysis did show that for the same frame, between-user selected rotation did vary by an average of $6.44^{o} \pm 3.01^{o}$. It is possible that for a single frame, this potential 9^{o} difference between users could lead to vastly different results. This analysis has not yet been completed and will be the focus on future studies.

With two potential sources of error from both the ultrasound technician and the between-user parameter selection variability, it is impossible to tell which one is the source of error in this study. More data is needed, holding each variable constant, to fully assess whether or not each potential source of variability has a significant effect on the final measured angle deviation and optimal ratio.

5 Conclusion

This preliminary analysis showed the ability to take qualitative VFI data for pediatric patients and, using a custom MATLAB script, quantify it and output the average angle deviation from theoretical healthy flow and the optimal major:minor axis ratio. This preliminary analysis showed that angle deviation is independent from age within the patient age group, weight, and heart rate ($p = 0.53$, $p = 0.50$, $p = 0.78$ respectively). This analysis also showed that the average angle deviation for 12 healthy patients was found to be $64.85^{o} \pm 10.34^{o}$ and the average optimal ratio was found to be 1.98 ± 0.58. As more patients are recruited into this clinical trial, a standard literature definition of flow deviation and optimal ratio can be defined for healthy patients. This standard literature definition can then be used to confirm patients expected of being diseased as truly having diseased flow, or conversely, as a method of screening out patients who are healthy from those who have disturbed ventricular flow dynamics. This information has the potential to give clinicians a better understanding of ventricular flow dynamics which could enable them to make earlier diagnoses and/or recommendations for treatment before noticeable anatomical remodeling has occurred.

Future studies will focus on error analysis and will work on reducing the source of user variability from the user interface end. This will be accomplished by adding better optimization features to the MATLAB code as well as performing directional statistics. There will also be the incorporation of more healthy patients to improve statistical conclusion validity, as well as the incorporation of unhealthy patients to assess whether or not there is a significant difference between the angle deviation between healthy patients and those with disturbed ventricular flow dynamics. The ultimate goal of this research is to provide a guideline for clinicians to follow when making decisions about the diagnosis and/or time of intervention for surgical intervention for pediatric patients with heart conditions based on their ventricular flow patterns.

6 References

Hansen, Kristoffer Lindskov, et al. “First Report on Intraoperative Vector Flow Imaging of the Heart among Patients with Healthy and Diseased Aortic Valves.” *Ultrasonics*, vol. 56, 2015, pp. 243–250., doi:10.1016/j.ultras.2014.07.015.

Hoffman, Julien I.E, and Samuel Kaplan. “The Incidence of Congenital Heart Disease.” *JACC*, Journal of the American College of Cardiology, 19 June 2002, www.onlinejacc.org/content/39/12/1890. Accessed 31 Mar. 2019.

Ii, R. Thomas Collins, et al. “Real-Time Transthoracic Vector Flow Imaging of the Heart in Pediatric Patients.” *Progress in Pediatric Cardiology*, 2019, doi:10.1016/j.ppedcard.2019.02.003.

Kilner, Philip J., et al. “Asymmetric Redirection of Flow through the Heart.” *Nature*, vol. 404, no. 6779, 2000, pp. 759–761., doi:10.1038/35008075.

Linde, Denise van der, et al. “Birth Prevalence of Congenital Heart Disease Worldwide.” *JACC*, Journal of the American College of Cardiology, 15 Nov. 2011, www.onlinejacc.org/content/58/21/2241. Accessed 31 Mar. 2019.

Munk, Peter, and Peter Munk. “A New Method for Estimation of Velocity Vectors.” *IEEE Transactions on Ultrasonics, Ferroelectrics and Frequency Control*, www.academia.edu/917365/A_new_method_for_estimation_of_velocity_vectors. Accessed 2 Apr. 2019.

Pedrizzetti, Gianni, and Federico Domenichini. “Nature Optimizes the Swirling Flow in the Human Left Ventricle.” *Physical Review Letters*, vol. 95, no. 10, 2005, doi:10.1103/physrevlett.95.108101.

Pedrizzetti, Gianni, et al. “The Vortex-an Early Predictor of Cardiovascular Outcome?” *Nature News*, Nature Publishing Group, 3 June 2014, www.nature.com/articles/nrcardio.2014.75. Accessed 31 Mar. 2019.

Sengupta, Partho P., et al. “Emerging Trends in CV Flow Visualization.” *JACC*, JACC: Cardiovascular Imaging, 1 Mar. 2012, imaging.onlinejacc.org/content/5/3/305. Accessed 1 Apr. 2019.